

Prediction of thermal effects on machine tool volumetric error

Martin Okénka, Jaromír Houša, Otakar Horejš, Martin Mareš, Martin Morávek

ČVUT v Praze, Fakulta strojní, Ústav výrobních strojů a zařízení, RCMT, Horská 3, 128 00 Praha 2, Česká republika

Abstract

Since a significant and possibly major part of machine tool error is caused by thermal deformation, its compensation has high priority as an accuracy increasing tool. Various methods of compensation have been developed including a dynamic method using transfer functions. Such a method, with relatively minor calibration requirements, is proven to be reliable in the prediction of thermally induced error at one point of a machine tool workspace. This paper focuses on extending the method usability across the workspace. A possibility of extrapolating the predicted deviation of a tool in the direction of Z axis in the calibrated location to the whole workspace is examined. The concept verification on data provided by recently developed volumetric measurement method is presented. Furthermore, data obtained by volumetric measurement of kinematically different machine tool are introduced.

Keywords: Thermal error; compensation; thermoelastic behaviour; volumetric compensation; position dependency

1. Introduction

Since the heat generated and accumulated in the machine tool (MT) and its surrounding induces significant displacement of the tool centre point (TCP), there is a number of methods developed to more or less successfully compensate for thermally induced error [1]. Passive methods such as thermally unresponsive or symmetric construction give limited results while being cost demanding. Active methods such as managing heat sources and sinks, active TCP position sensing, multi linear regression models or FEM based models offer partial solutions. However, cost effectiveness, robustness and ease of implementation are issues.

High quality thermal error compensation offers a transfer function (TF) based model while using no additional gauges and being easy to calibrate and integrate to a control system of a MT. A TF model was described in [2] and proven to be capable of high quality and robust thermal error compensation in the calibration point of the workspace of various types of MTs [3].

The major contribution to overall thermally induced error is distortion caused by heat produced by a rotating spindle [2]. According to the measurement carried out in [4], the error caused by the rotating spindle is articulated primarily in the direction of the rotational axis (Z). The paper also presented the inequality of the thermally induced error across the workspace of a MT. Thus the one point TF models (standard TF models) harbour an improvement potential.

2. Experimental setup

The experiment described subsequently aims to extrapolate the error estimation given by the standard TF model to the whole MT workspace using a low order relation to a motion axis position. The only applied load is spindle rotation and the investigated error is in Z direction since those are the main error source and the most significant error component [4], [5]. Additionally, as error caused by

spindle rotation does not vary significantly over the workspace of mid-sized MTs, the measurement for the extrapolation verification took place on a heavy floor type MT (see Figure 1 depicting kinematic configuration of the floor type MT and placement of the temperature sensors).

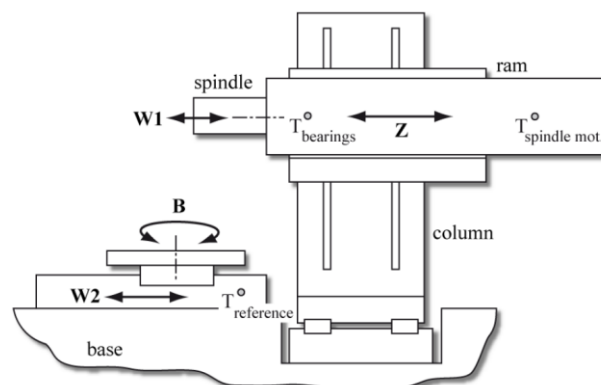


Figure 1. Kinematic configuration of a floor type MT with marked temperature sensor positions, [2]

Due to serial configuration of the MT, an approximately linear distribution of TCP position error may be assumed and, furthermore, the dependency on X axis position should be limited as the X guideway is on a long and robust bed far from the heat source. Thus only Y and Z position are used for the extrapolation.

In Figure 2, the measuring device is depicted; calibrated spheres are placed across the workspace and periodically located using a self-centring probe “MT-Check” (see [4], [5] for further details of the measurement method and the device).

When the MT is in thermo-dynamic equilibrium with its surrounding, spindle rotation is set to a constant speed and the displacement of the TCP is recorded at the coordinates of individual spheres during the heating process. The coordinates are given in Table 1, Figure 3 depicts their positions in the workspace graphically.

* Contact details: M.Okenka@rcmt.cvut.cz

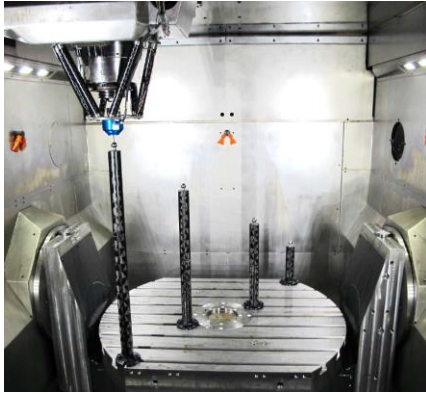


Figure 2. Volumetric error measuring of 5-axis machining centre using MT-Check probe and calibrated spheres placed across the workspace [5]

Table 1. Position of individual reference spheres

Sphere num.	X	Y	Z
	[mm]		
1	2628	-794	-1126
2	2628	-1441	-1112
3	2633	-2111	-1108
4	3026	-1731	-620
5	3220	-789	-416
6	3225	-2111	-412

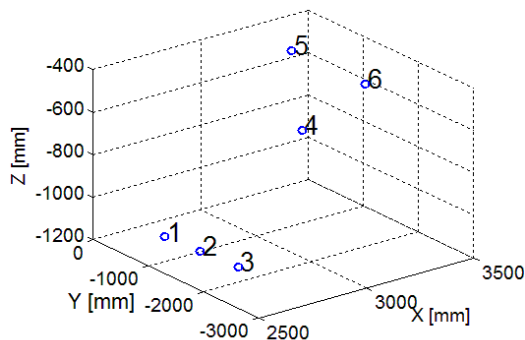


Figure 3. Plotted position of individual reference spheres

Simultaneously with the TCP position measurement, a temperature sampling took place at both the MT spindle and surroundings (Figure 1: $T_{\text{spindle mot.}}$ and $T_{\text{reference}}$). Both the TCP error and temperatures were recorded on a MT thermally loaded by free spindle rotation at speed of 500 rpm and 2000 rpm respectively.

3. Calibration and modelling

Extrapolation of the predicted error from one point to the whole workspace is based on the assumption of linear thermal error dependency on the motion axis position. Therefore, the ratio b of given deformations at individual coordinates should be a constant and the following relation would describe the deformation across the workspace:

$$\Delta Z_j = b_j \Delta Z_{\text{cal}} \quad (1)$$

where ΔZ stands for the time vector of the Z deformation at point j , b_j for linear coefficient and ΔZ_{cal} stands for the

time vector of predicted deformation of the TCP at the point of calibration of the TF model.

Once the coefficients b_j are known at a number of different coordinates of the workspace, it is possible to obtain its value at an arbitrary point of the workspace by linear interpolation. To minimize calibration requirements, 4 of the measured points were chosen to obtain corresponding b_j coefficients (spheres number 1, 3, 5, 6 in Figure 3). Points number 4 and 6 serve as control points for interpolation. The TF model was calibrated at point 4 (based on test with spindle rotational speed of 500 rpm).

The TF model extrapolation is then verified under non-calibration conditions (tested with spindle rotational speed of 2000 rpm).

For practical thermal error compensation, a more complex TF model is needed, covering differences of heating and cooling processes and respecting alternations of the thermal MT behaviour due to various thermal loads. Nevertheless, the aim of this research is to investigate regularity of error dispersion due to thermal load of the rotating spindle. Thus only the heating process is taken into consideration. Concept of the TF model itself has been proved [3].

First, the one-point TF model was calibrated at point number 4 on the MT loaded by spindle rotation of 500 rpm. The only inputs used for the model are temperatures of the spindle motor and the MT surroundings ($T_{\text{spindle mot.}}$, $T_{\text{reference}}$). See Figure 4 comparing the measured value of Z deformation at the point 4 and the value predicted by TF model. The model follows the measured data perfectly and under similar conditions should provide solid source data for extrapolation to the MT workspace.

The norm *fit* (eq. 2) is used to quantify the quality of the estimation:

$$fit_j = \left(1 - \frac{\|\Delta Z_j - \overline{\Delta Z_j}\|}{\|\Delta Z_j - \Delta Z_j\|} \right) \cdot 100 \quad (2)$$

where ΔZ_j stands for measured value of Z deformation, $\overline{\Delta Z_j}$ for its arithmetic mean over time and $\widehat{\Delta Z_j}$ stands for the value estimated by the TF model or its extrapolation, $\|\mathbf{x}\|$ marks Euclidean norm.

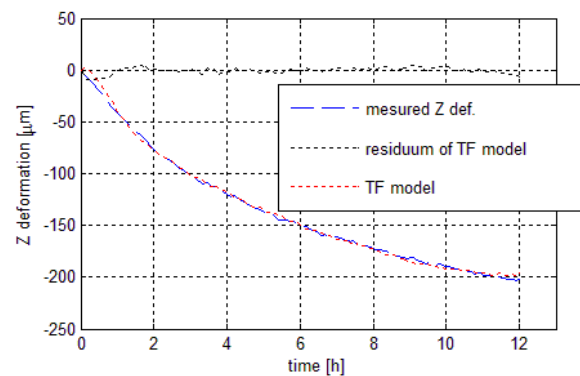


Figure 4. Measured Z component of deformation at point 4 compared to value predicted by the TF model calibrated at the same point, black dotted line marks difference (residual error), $fit = 94.4\%$

3.1 Extrapolation

For extrapolation of the deformation predicted by the standard TF model (see Figure 4), the b_j coefficients were obtained from measured data as arithmetic mean over time of ratio of Z deformation of individual spheres to Z deformation of the sphere number 4 (eq. 1, Figure 3). The b_j values are presented in Table 2 for test with constant spindle rotation of 500 rpm. Note that the ratios of Z deformation of individual spheres are close to 1. Nevertheless compensating for those residual differences might further improve performance of single point models in MT workspace by avoiding such divergence.

Table 2. Value of coefficients b_j for individual measuring spheres for 500 rpm

Ball nr. "j"	1	2	3	4	5	6
$b_{j\ 500}$	1.14	1.14	1.08	1	0.97	0.9

By multiplying the predicted value of the TF model (Figure 4) by the corresponding b_j (Table 2) accordingly to eq. 1, the extrapolated values can be plotted and compared to values measured at each point and to the value given by the standard TF model.

For corner spheres, the extrapolated value uses directly the known coefficients (Figures 5; spheres a) 1, b) 3, c) 5, d) 6; coefficients b_1, b_3, b_5, b_6). Values for intermediate spheres (Figure 6; spheres a) 2 and b) 4) use coefficients obtained by linear interpolation from the corner four ones.

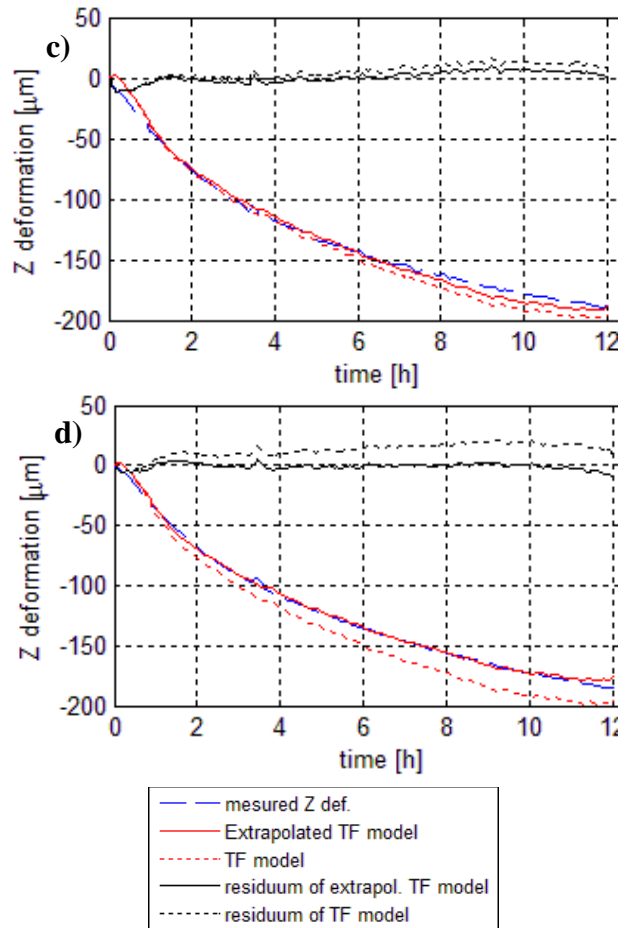
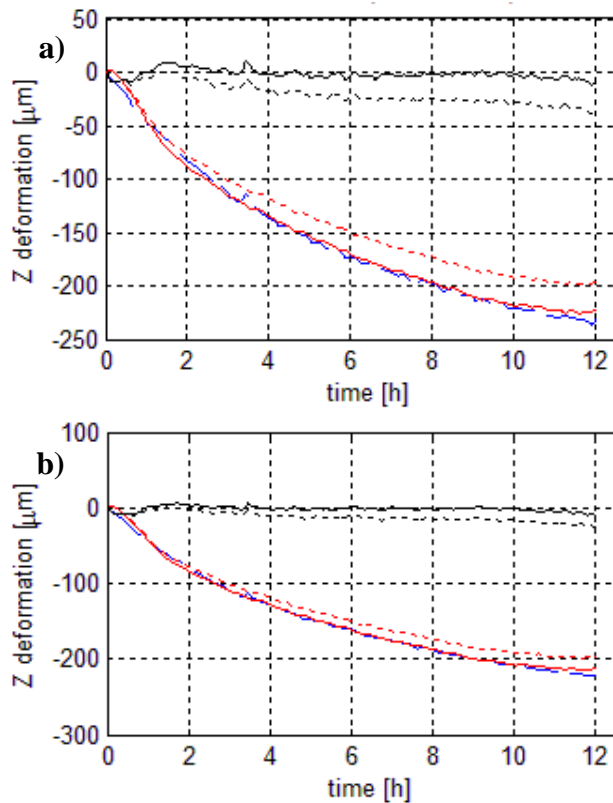
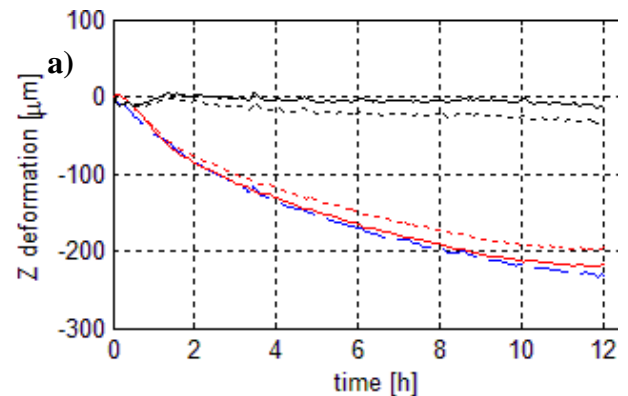


Figure 5. Z deformation vs. time compared to extrapolated and standard TF model, accompanied by corresponding residua for individual spheres; 500 rpm; linear coefficients directly experimentally identified (Table 2)

- a) Sphere 1 b) Sphere 3
- c) Sphere 5 d) Sphere 6



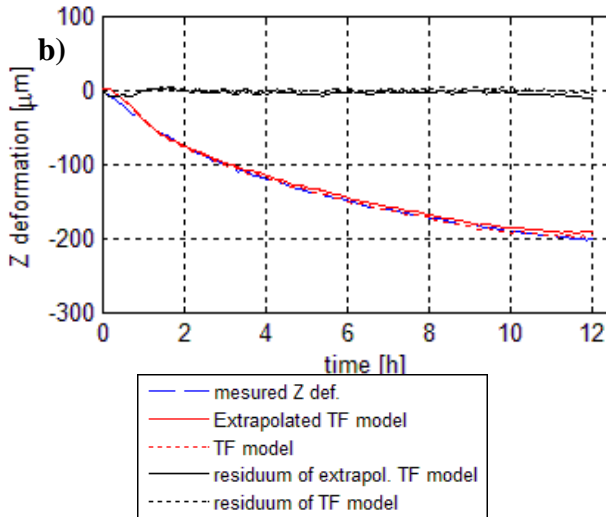


Figure 6. Z deformation vs. time, 500 rpm; linear coefficients interpolated from corner spheres

a) Sphere 2 b) Sphere 4 (calibration point of TF model)

Note that while the shape of the deformation progress is well estimated by the standard TF model, the absolute values are not met perfectly except for the calibration point. After compensation with the help of the model extrapolation (eq. 1) both the shape of error evolution and its absolute value are well estimated.

For residual error quantification, the peak-to-peak criterion (PK) is used as defined by following eq. 3.

$$PK = |\max(\Delta Z - \widehat{\Delta Z}) - \min(\Delta Z - \widehat{\Delta Z})| \quad (3)$$

The extrapolated fit values are compared to the fit values obtained by the standard TF model in Table 3. Note that for all but the calibration point, the fit value is evidently increased. Peak-to-peak values are presented on the right side of the Table 3 alongside with the maximum residual error (PK values) in terms of percentage of the uncompensated error ($\max|\Delta Z|$). Note that the extrapolation coefficients for spheres number 2 and 4 used are not the ones directly identified, but are interpolated from the corner spheres. Since the prediction quality at points 2 and 4 is not significantly worsened, one can assume that the linear error distribution assumption is justifiable for measured case.

Table 3. fit values and PK values for standard TF model and its extrapolation, applied load – 500 rpm, symbol PK stands for peak-to-peak value of the residual error, subscript std TF stands for standard TF model, ext for its extrapolation

500 rpm	fit_{ext}	$fit_{std TF}$	PK_{ext}	$\frac{PK_{ext}}{\max \Delta Z }$	$PK_{std TF}$	$\frac{PK_{std TF}}{\max \Delta Z }$
sphere	[%]		[μm]	[%]	[μm]	[%]
1	92.7	65.5	27.4	11.9	41.6	18.1
2	89.9	66.7	29.1	12.6	40.2	17.5
3	93.9	77.9	18.5	8.4	28.9	13.1
4	90.5	94.4	16.5	8.3	17.0	8.5
5	90.4	83.3	24.5	13.2	31.0	16.8
6	94.8	72.2	16.0	8.7	29.9	16.3
average	92	77	22.0	10.5	31.4	15.0

4. Verification

The error estimation of the MT loaded by 2000 rpm was carried out to investigate the quality of TF model and its extrapolation under non-calibration conditions. Figure 7 a) depicts the best obtained result (on sphere 1) and Figure 7 b) the worst (on sphere 6). Table 4 shows fit values for standard TF model and its extrapolation and the residual error in terms of percentage of the uncompensated error.

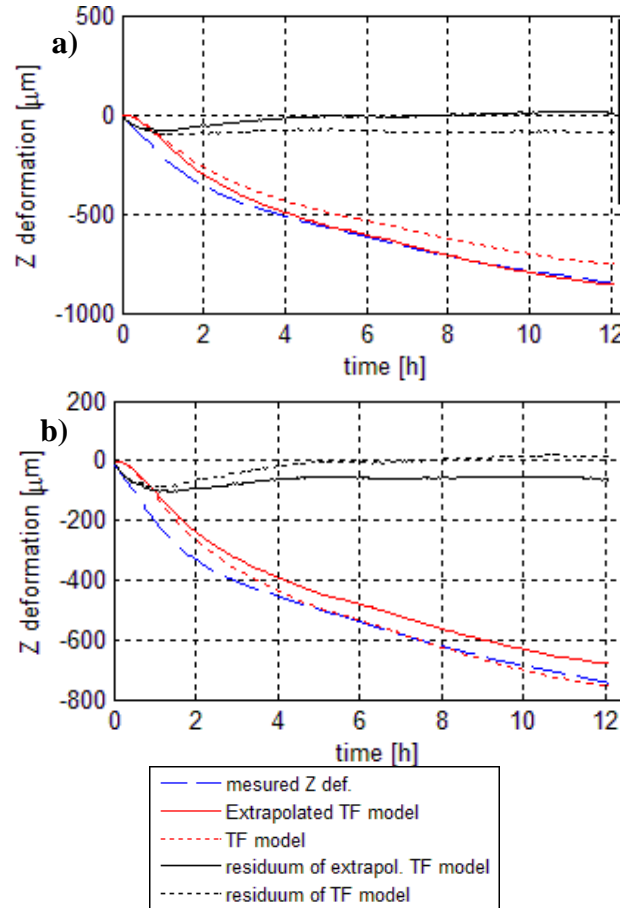


Figure 7. Z deformation vs. time, 2000 rpm

a) Sphere 5 – the best fit b) Sphere 6 – the worst fit

Table 4. fit values and PK values for the standard TF model and its extrapolation, applied load – 2000 rpm

2000 rpm	fit_{ext}	$fit_{std TF}$	PK_{ext}	$\frac{PK_{ext}}{\max \Delta Z }$	$PK_{std TF}$	$\frac{PK_{std TF}}{\max \Delta Z }$
sphere	[%]		[μm]	[%]	[μm]	[%]
1	84.7	60.2	105.8	12.6	104.0	12.4
2	81.5	59.7	94.5	11.2	107.9	12.8
3	78.1	61.2	94.4	11.2	105.8	12.6
4	68.8	74.5	105.1	13.6	101.3	13.2
5	80.1	81.6	95.3	13.1	115.7	16.0
6	63.0	79.9	106.1	14.5	113.4	15.5
average	76	70	100.2	12.7	108.0	13.7

The TF model calibrated under 500 rpm is not capable of capturing the physical nature of heat progression for higher loads. Neither the absolute values of the TCP deformation nor the shape of the error development matches the measured values. Moreover, the used b_j (calibrated for 500 rpm) does not respect volumetric variance of the

deformation. Thus estimated values do not match the measured values as closely as at 500 rpm. Still, a remarkable error compensation was obtained even in the worst case (average error reduction from $792 \mu\text{m}$ to $100.2 \mu\text{m}$).

5. Results

The extrapolation method described enables the standard one-point TF model for thermal error compensation to be used throughout the whole workspace. The thermal error time development due to a rotating spindle was found similar in shape across the workspace of the MT. Thus linear coefficients b_j facilitate residual error minimization.

Under calibrating conditions of the TF model and of the b_j , the *fit* value was increased by the extrapolation to over 90 % and the residual error was reduced to less than or equal to $29 \mu\text{m}$ (non-compensated error over $200 \mu\text{m}$). The results under calibration conditions show that the assumption of (time consistently) linear error distribution can be utilised to expand the usability of standard compensation models.

The b_j values were not satisfactorily proven to be valid under conditions far from calibration since the TF model extrapolation did not enhance standard TF model performance across the whole workspace. While extrapolation decreased the approximation quality for spheres 4, 5, 6, it managed to limit the residual error under $106 \mu\text{m}$ (non-compensated error over $800 \mu\text{m}$, standard TF model compensated error $104\sim 115 \mu\text{m}$). While the b_j is time consistent, it varies depending on the applied thermal load. Therefore multiple values should be identified for individual basic load spectra. A new values of $b_{j\ 2000}$ calibrated under high revolutions are presented in Table 5 accompanied with reached *fit* and *PK* (peak-to-peak of residual error) values.

Table 5. Value of coefficients b_j for individual measuring spheres for 2000 rpm test accompanied with reached *fit* and *PK* values

Ball nr. "j"	1	2	3	4	5	6	avg.
$b_{j\ 2000}$	1.06	1.07	1.06	1	0.93	0.96	
<i>fit</i> [%]	74.2	73.6	75.2	71.3	73.3	75.6	73.9
$PK_{ext\ 2000}$ [μm]	95.3	99.7	96.2	103.5	93.8	97.3	97.6

A comparison of Table 2 with Table 5 shows that the dependency on the motion axis position is reduced for higher revolutions. Additionally, comparison of Table 4 and Table 5 yields that the proprietary $b_{j\ 2000}$ does not compensate for an insufficiently estimated evolution of the TCP displacement by the TF model (calibrated under 500 rpm). Nevertheless, a further reduction of the residual error from avg. $100.2 \mu\text{m}$ to $97.6 \mu\text{m}$ was obtained using the dedicated $b_{j\ 2000}$. This indicates that every TF model for specified conditions (high/low revolution, heating/cooling) should be accompanied by proprietary b_j values. With such a combination, presumably the *fit* value attained may reach over 90 % for high revolutions as for low revolutions.

Above presented data show that the assumption of linearly distributed thermal error caused by spindle rotation is viable mean of the volumetric model complexity reduction for given type of MT. If instead of the described extrapolation a grid of multiple standard TF models is used to reflect the volumetric dependency of thermal error, presented results show a low density grid (i.e. a face-centred cubic distribution) should be sufficient.

6. Application on other kinematics

To investigate presented outcome on non-purely serial kinematics, volumetric error of multifunctional turning centre (Figure 8) was measured. Basic overview of said experiment follows in subsequent sections.

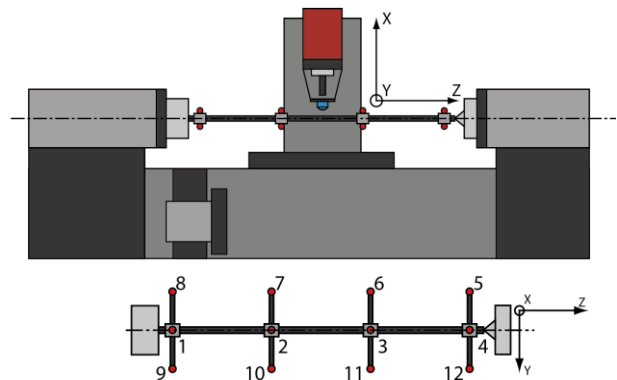


Figure 8. Partially parallel structure of multifunctional turning centre with MT-Check probe on milling head and frame with numbered reference spheres clamped in turning chuck (and supported by tailstock centre)

6.1. Experimental setup

The turning centre was fitted with reference spheres on frame between turning chuck and tailstock centre (Figure 8). The spheres were periodically located using the MT-Check probe mounted on milling headstock while the MT was under thermal load of rotating milling spindle (2000 rpm). Let us focus on deformation in X direction (axis of rotating spindle) as in previous case.

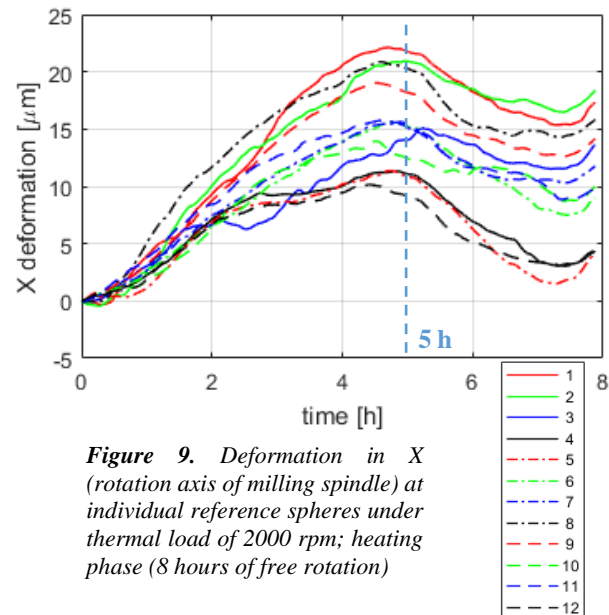


Figure 9. Deformation in X (rotation axis of milling spindle) at individual reference spheres under thermal load of 2000 rpm; heating phase (8 hours of free rotation)

Figure 9 shows deformation in X direction of MT structure under thermal load of freely rotating milling spindle at individual reference spheres (heating phase only: 8 hours of 2000 rpm). And Figure 9 shows its volumetric interpretation at time 5 hours (marked in Figure 8).

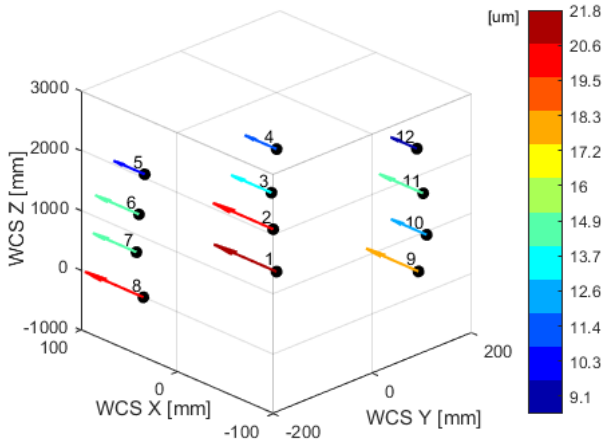


Figure 9. X deformation at individual reference spheres after 5 hours of thermal load (milling spindle at 2000 rpm)

The presented data evidently show the necessity of positional dependent modelling of thermal error as its difference across the workspace is over 100 % (i.e. spheres number 1 and 12).

Since the deformation curves are loosely comparable and primarily differ in amplitude, the above described extrapolation method can be expected to improve performance of the standard TF model. Yet the ratio between deformations at individual measuring points is not time consistent and thus multiple individual TF models independently calibrated at each measured point should provide superior quality of prediction. The presented data give us insight on how dense the grid of independent TF models should be.

7. Conclusion

The presented method of extrapolation the standard TF model using linear coefficients improved the prediction quality across the workspace of investigated MT under calibrating condition. Detailed summary of the method performance is given in chapter 5.

The major outcome of the experiment is that every load spectrum should be associated with designated TF model and set of extrapolating coefficients. Considering the measured deformation on turning centre which did not prove to be time-consistently linearly dependent, a more rigid and universal approach of volumetric grid of multiple TF models can be proposed. Such approach does not require more extensive calibration measurement while being able to describe the time dependant variation of volumetric error.

Presented data show that the grid density of TF models for proposed method can be relatively small (3x3x3 or in form of face centred cube) which keeps the calibration requirements on acceptable level.

Future work in this vein should explore the possibility of proposed method, concentrate on including more thermal sinks and sources (axis movement) and incorporate

compensation in all directions. The portfolio of heavy-duty MTs with advanced thermal error compensation models should be further extended.

Acknowledgements

This research (Prediction of thermal effects on machine tool volumetric error) has received funding from the Technology Agency of the Czech republic (Project (TE01020075)).

Symbols

b_j	linear extrapolation coefficient of j^{th} reference sphere (1)
fit	norm defined by (eq. 2) used to quantify the quality of the estimation (%)
PK	peak-to-peak criterion of residual error defined by (eq. 2) (μm)
T	temperature (K)
ΔZ_j	time vector of displacement in Z direction of j^{th} reference sphere (μm)
ΔZ_{cal}	time vector of displacement in Z direction of TF model calibrating sphere (μm)
$\widehat{\Delta Z}_j$	time vector of displacement estimated by the TF model or its extrapolation at j^{th} sphere (μm)
$\overline{\Delta Z}_j$	arithmetic mean over time of time vector of measured displacement at j^{th} sphere (μm)

Subscripts

ext	related to extrapolated values
$std TF$	related to standard TF model values
500	related to calibrating conditions of 500 rpm
2000	related to calibrating conditions of 2000 rpm

Reference

1. J. Mayr, J. Jedrzejewski, E. Uhlmann, M. Alkan Donmez, W. Knapp, F. Härtig, K. Wendt, T. Moriwaki, P. Shore, R. Schmitt, C. Brecher, T. Würz a K. Wegener, Thermal issues in machine tools, CIRP Ann.Manuf.Technol., Vol.. 61, n. 2, p. 771–791, 2012.
2. Mareš, M., Horejš, O., Hornych, J., Advanced Thermal Error Compensation of a Floor Type Machining Centre Allowing for the Influence of Interchangeable Spindle Heads. Journal of Machine Engineering, 2015, Vol. 15, No. 3, p. 19-32. ISSN 1895-7595.
3. Horejš, O., Mareš, M., Hornych, J., Thermal error compensation models based on transfer functions of different machine tool structures. In: EUSPEN Special Interest Group: Thermal Issues, 19-20 March 2014, Zurich, Switzerland.
4. Morávek, M., Bureš, J., Horejš, O., Volumetric measurement of machine tool thermal deformation using an MT-Check probe. In: 11th International Conference and Exhibition on Laser Metrology, Huddersfield, UK, 2015.
5. Morávek, M., Horejš, O., Volumetric Measurement of Five-axis Machine Tool Thermal Deformation Using an MT-Check Probe. In: EUSPEN Special Interest Group: Thermal Issues, 17-18 March 2016, Prague, Czech Republic.